HRAS Mutation Prevalence and Associated Expression Patterns in Pheochromocytoma

Adam Stenman,[1,2]* **Jenny Welander,**[3] **Ida Gustavsson,**[3] **Laurent Brunaud,**[4] **Martin Bäckdahl,**[5]
Peter Söderkvist,[3] **Oliver Gimm,**[3,6] **C. Christofer Juhlin,**[1,2] **and Catharina Larsson**[1,2]

[1]Department of Oncology and Pathology, Karolinska Institutet, Stockholm, SE-17176, Sweden
[2]Cancer Center Karolinska, CCK, Karolinska University Hospital Solna, Stockholm, SE-171 76, Sweden
[3]Department of Clinical and Experimental Medicine, Faculty of Health Sciences, Linköping University, Linköping, SE-581 85, Sweden
[4]Department of Digestive, Hepato-Biliary and Endocrine Surgery, CHU Nancy – Hospital Brabois Adultes, University De Lorraine, Vandoeuvre-les-Nancy, F-54511, France
[5]Department of Molecular Medicine and Surgery, Karolinska Institutet, Stockholm, SE-171 76, Sweden
[6]Department of Surgery, Region Östergötland, Linköping, SE-58185, Sweden

Pheochromocytomas (PCC) and abdominal paragangliomas (PGL) display a highly diverse genetic background and recent gene expression profiling studies have shown that PCC and PGL (together PPGL) alter either kinase signaling pathways or the pseudo-hypoxia response pathway dependent of the genetic composition. Recurrent mutations in the *Harvey rat sarcoma viral oncogene homolog* (*HRAS*) have recently been verified in sporadic PPGLs. In order to further establish the *HRAS* mutation frequency and to characterize the associated expression profiles of *HRAS* mutated tumors, 156 PPGLs for exon 2 and 3 hotspot mutations in the *HRAS* gene was screened, and compared with microarray-based gene expression profiles for 93 of the cases. The activating *HRAS* mutations G13R, Q61R, and Q61K were found in 10/142 PCC (7.0%) and a Q61L mutation was revealed in 1/14 PGL (7.1%). All *HRAS* mutated cases included in the mRNA expression profiling grouped in Cluster 2, and 21 transcripts were identified as altered when comparing the mutated tumors with 91 *HRAS* wild-type PPGL. Somatic *HRAS* mutations were not revealed in cases with known PPGL susceptibility gene mutations and all *HRAS* mutated cases were benign. The *HRAS* mutation prevalence of all PPGL published up to date is 5.2% (49/950), and 8.8% (48/548) among cases without a known PPGL susceptibility gene mutation. The findings support a role of *HRAS* mutations as a somatic driver event in benign PPGL without other known susceptibility gene mutations. *HRAS* mutated PPGL cluster together with *NF1*- and *RET*-mutated tumors associated with activation of kinase-signaling pathways.   © 2016 The Authors Genes, Chromosomes & Cancer Published by Wiley Periodicals, Inc.

INTRODUCTION

Pheochromocytomas (PCCs) and abdominal paragangliomas (PGLs), together abbreviated PPGL, are neuroendocrine tumors of the adrenal medulla and extra-adrenal paraganglia, respectively, displaying a highly heterogeneous genetic background (Dahia, 2014). Although the majority of cases are benign, significant subsets of PGLs are malignant and often associated with inactivating *SDHB* gene mutations. Recent studies have revealed that approximately 40% of PPGL patients carry a constitutional mutation in a susceptibility gene, and somatic mutations are found in an additional 30% of the tumors (Dahia, 2014). The currently known susceptibility genes include *NF1, RET, VHL, SDHA, SDHB, SDHC, SDHD, SDHAF2, EGLN1, EPAS1, FH* (Letouzé et al., 2013), *KIF1Bb* (Schlisio et al., 2008), *MAX* (Comino-Méndez et al., 2011), and *TMEM127* (Dahia, 2014). Single families with PPGL and a constitutional mutation in one of the genes *BAP1* (Wadt et al., 2012) and *MDH2* (Cascón et al., 2015) have

also been reported. The known genetic background of PPGL further includes a set of genes that are recurrently mutated in PPGL tumors such as *ATRX* (Fishbein et al., 2015), *KMT2D* (Juhlin et al., 2015), *MET* (Castro-Vega et al., 2015), *BRAF* (Luchetti et al., 2015), the *TERT* promoter (Liu et al., 2014), and *HRAS* (Yoshimoto et al., 1992; Crona et al., 2013). Expressional profiling studies of PPGL have

shown that tumors fall into two main clusters depending on their genetic composition (Dahia et al., 2005; Burnichon et al., 2011). Cluster 1 with *VHL*, *SDHx* and *EPAS1* mutated tumors is characterized by a pseudo-hypoxic response and Cluster 2 includes tumors with mutations in *MAX*, *NF1*, *RET*, and *TMEM127* that are associated with active kinase-signaling pathways (Dahia et al., 2005).

Somatic mutations in the *Harvey rat sarcoma viral oncogene homolog (HRAS)* gene were first reported in a single pheochromocytoma (Yoshimoto et al., 1992), and *HRAS* was more recently verified as a recurrently mutated gene in PCC. However, the two other members of the RAS family, that is, *NRAS* and *KRAS* have not been reported to be mutated in PPGL. Crona et al. identified *HRAS* mutations via exome sequencing and reported 3 mutated PCCs and 1 PGL (Crona et al., 2013). Oudijk and co-workers subsequently detected *HRAS* mutations in 5.2% of cases (14/271 PCCs) and proposed that the mutations are restricted to sporadic PCCs (10%, 14/140) (Oudijk et al., 2014) and Luchetti et al. published *HRAS* mutations in 6/65 PPGL (9.2%) (Luchetti et al., 2015). Recently, in a multiomics study by Castro-Vega et al. the authors screened 193 PPGL for *HRAS* mutations and found 10 mutated cases, all in benign, sporadic PPGL (Castro-Vega et al., 2015). Additionally, de Cubas et al. have mentioned 4 *HRAS*-mutated PPGL among 156 cases screened, whereof one mutation was found in a metastatic PPGL (de Cubas et al., 2015). Mutations at the hotspots codons 13 and 61 activate the transforming properties of various tumor types, and hence these recurrent mutations are thought to propagate PPGL tumorigenesis for a subset of cases. Germ-line *HRAS* mutations have been associated with the Costello syndrome, but to date no co-occurrence of this syndrome and PPGL has been reported (Crona et al., 2013; Luchetti et al., 2015). In this study, we aimed to further establish the *HRAS* mutation prevalence as well as its possible impact on global mRNA expression profiles in *HRAS* mutated PPGL.

MATERIALS AND METHODS

Pheochromocytoma and Paraganglioma (PPGL) Tumor Samples

A total of 156 PPGL (142 PCCs and 14 PGLs) were collected from Karolinska University Hospital, Stockholm, Sweden (Series A; *n* = 75), University de Lorraine, Vandoeuvre-les-Nancy, France (Series B, *n* = 60), Linköping University Hospital, Sweden

(Series C, *n* = 12), and Haukeland University Hospital in Bergen, Norway (Series D, *n* = 9), (Supporting Information Table 1). Samples were obtained with informed patient consent and with approval from the local ethics committee of the respective centers. Tumors were classified as benign or malignant following the WHO criteria (DeLellis et al., 2004). For Series A, a subset of the tumors (*n* = 54) had been characterized for mutations in 14 proposed PPGL susceptibility genes (*EGLN1*, *EPAS1* *KIF1Bβ*, *MAX*, *MEN1*, *NF1*, *RET*, *SDHA*, *SDHB*, *SDHC*, *SDHD*, *SDHAF2*, *TMEM127*, and *VHL*) (Welander et al., 2014a) and the remaining tumors (*n* = 21) were screened for mutations in 8 of these genes (*EPAS1*, *MAX*, *NF1*, *SDHB*, *SDHD*, *RET*, *TMEM127*, and *VHL*) (Welander et al., 2014b) (Supporting Information Table 1). Furthermore, all tumors in Series C and D were previously analyzed for mutations in the 8 genes (*EPAS1, MAX, NF1, SDHB, SDHD, RET, TMEM127*, and *VHL*) (Welander et al., 2014b) (Supporting Information Table 1). For Series B, a subset of patients exhibited established PPGL syndromes with associated mutations (Supporting Information Table 1).

HRAS Mutation Analysis

Genomic DNA isolated from fresh frozen tumor samples was used for amplification of fragments of exon 2 and 3 covering codons 13 and 61 of the *HRAS* gene (NM_001130442) with primer sequences available upon request. Sanger sequencing was carried out at the KIGene core facility at Karolinska Institutet for 113 cases and at Linköping University for 42 cases using previously described methodology (Welander et al., 2014a). All samples showing chromatogram alterations were re-analyzed with the reverse primer. One *HRAS* mutation (case 88) has been previously reported and was found via whole-exome sequencing (Supporting Information Table 1) (Juhlin et al., 2015).

Gene Expression Profiling

Total RNA was extracted from 53 PPGLs from Series A (Supporting Information Table 1), using the mirVana Isolation Kit (Ambion, Austin, TX) and subsequently analyzed in an Agilent 2100 Bioanalyzer (Agilent, Santa Clara, CA). As previously reported, RNA preparations from all cases were of sufficient quality as measured by RIN values (Andreasson et al., 2013a,b). RNA samples (250 ng) were used for whole-transcriptome analysis with GeneChip Human Gene 1.0 ST arrays (Affymetrix),
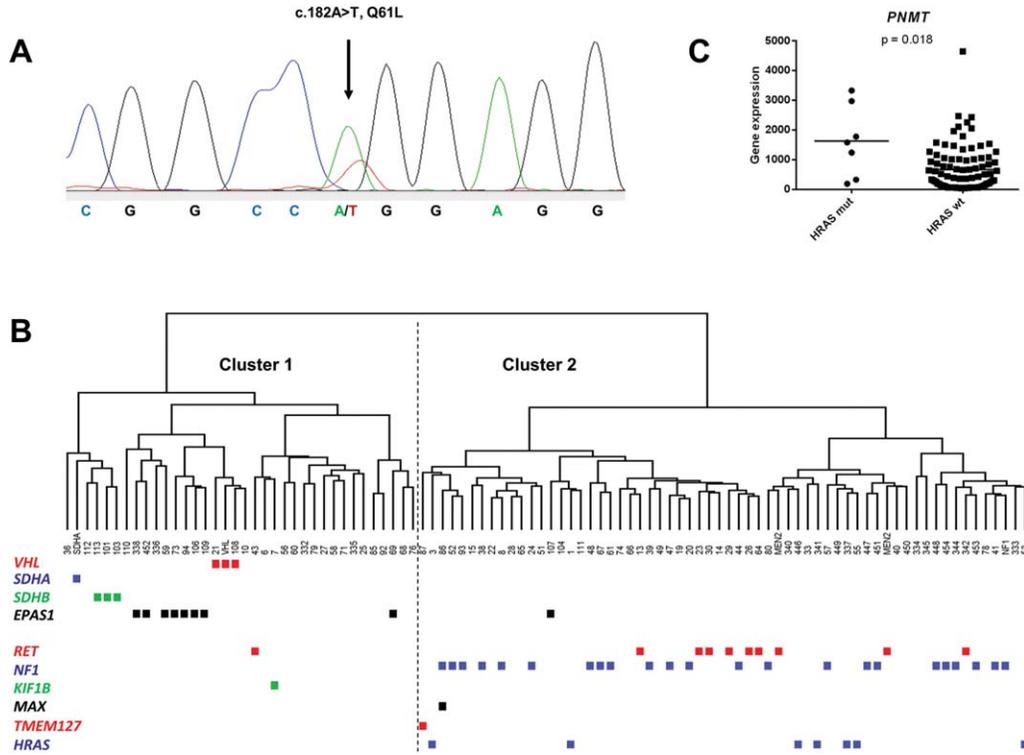
Figure 1. Detection of a *HRAS* Q61L mutation, hierarchical clustering of PPGLs and *PNMT* gene expression in relation to *HRAS* mutation status. **(A)** Chromatogram of case 227 (PGL) showing the Q61L mutation (c.182A>T, COSM498), which has previously not been reported in PPGL. A vertical arrow shows the heterozygous missense variant. **(B)** Hierarchical clustering of 93 tumors (indicated by their case numbers) and 5 control cases (indicated as MEN2, NF1, SDHA, and VHL) based on their expression levels for 454 genes according to Burnichon et al. 2011. The dendrogram shows separation of tumors into two distinct groups (Cluster 1 to the left and Cluster 2 to the right). The PPGL mutation status is indicated below. All 7 *HRAS*-mutated cases clustered together with the tumors endowed with mutations in the *NF1-* and *RET* genes. **(C)** RNA levels of the *PNMT* gene compared between the PPGL with (*HRAS* mutated $n = 7$) and without (*HRAS* wild-type $n = 86$) *HRAS* mutations. Horizontal bars represent mean values and the gene expression has been normalized to the mean value of cases endowed with constitutional *NF1-* and *RET* mutations. [Color figure can be viewed in the online issue, which is available at wileyonlinelibrary.com.]

covering approximately 29K annotated genes as previously described (Welander et al., 2014b). Tumor RNA from 40 cases in Series A–C (detailed in Supporting Information Table 1) had previously been analyzed with the GeneChip Human 1.0 ST array (Affymetrix) (Welander et al., 2014b). *HRAS* mutation status from the current study was implemented into the dataset and after normalization using the robust multiarray average (RMA) algorithm, hierarchical clustering of the microarray expression data for all 93 PPGLs was performed as previously described (Welander et al., 2014b) using a set of genes that has been shown to separate the clusters (Burnichon et al., 2011). These genes overlapped with 454 of the probe sets in our analysis which were used to perform the hierarchical clustering. Moreover, gene expression profiles based on the entire probe sets on the array were compared between the 7 *HRAS* mutated cases and the 91 *HRAS* wild-type cases included. Given their involvement in PPGL, normalized signal intensities for the *HRAS*, *vascular endothelial growth factor A* (*VEGFA*) and *phenylethanolamine*

N-methyltransferase (*PNMT*) genes were exported for separate statistical analysis.

Within the cohort, tumors with known somatic mutations in *EPAS1, KIF1Bb, MAX, NF1, RET, SDHA, SDHB, TMEM127*, and *VHL* were included (Supporting Information Table 1). Additionally, five cases from patients with known PPGL syndromes (2 MEN2, 1 NF1, 1 PGL5, and 1 VHL) were included as internal controls and were also included in the hierarchical clustering. One identical sample was analyzed at both time points in (Welander et al., 2014b) and in the current study as an internal control between the GeneChip arrays. This sample did not show any difference in clustering behavior as evaluated with a principal component analysis quality control in the GeneSpring software (data not shown).

Statistical Analyses

Transcriptome-wide statistical analyses and clustering were performed as previously described

TABLE 1. HRAS Gene Mutations and Clinical Characteristics of the PPGL Included in the Study

Parameter	Series A	Series B	Series C	Series D	Series A, B, C, and D
Gender					
Male:Female	32:43	26:34	5:7	3:6	66:90
Age at diagnosis					
Mean years	55	53	63	58	55
Median (range) years	57 (14–83)	52 (23–84)	66 (39–76)	58 (42–80)	57 (14–84)
Tumor type					
Total	75	60	12	9	156
PCC	64	57	12	9	142
PGL	11	3	0	0	14
Tumor size					
Mean mm	52	41	34	47	46
Median (range) mm	45 (20–160)	40 (10–100)	30 (17–60)	50 (10–90)	40 (10–160)
Malignancy					
Benign	69	59	12	9	149
Malignant	6	1	0	0	7
PPGL susceptibility gene					
Mutated	37	9	3	6	55
Unknown mutation (sporadic)	38	51	9	3	101
HRAS codon 13 and 61					
Wild-type	70	57	10	8	145
Mutated	5	3	2	1	11
G13R	0	0	1	0	1
Q61R	3	1	1	1	6
Q61K	2	1	0	0	3
Q61L	0	1 (PGL)	0	0	1
HRAS mutation frequencies					
Total	6.7%	5.0%	16.7%	11.1%	11/156 (7.1%)
PCC	7.8%	1.5%	16.7%	11.1%	10/142 (7.0%)
PGL	0%	33.3%	0%	0%	1/14 (7.1%)
According to gender					
Male	6.3%	7.7%	0%	0%	4/66 (6.1%)
Female	7.0%	2.9%	28.6%	16.7%	7/90 (7.8%)
According to malignancy					
benign	7.2%	5.1%	16.7%	11.1%	11/149 (7.4%)
Malignant	0%	0%	0%	0%	0/7 (0%)
According to susceptibility gene status					
Unknown mutation (sporadic)	13.2%	5.9%	22.2%	33.3%	11/101 (10.9%)
Mutated	0%	0%	0%	0%	0/55 (0%)

Tumor size refer to the maximum diameter.
Series A = Karolinska University Hospital, Sweden.
Series B = University de Lorraine, Vandoeuvre-les-Nancy, France.
Series C = Linköping University Hospital, Linköping, Sweden.
Series D = Haukeland University Hospital, Bergen, Norway.

(Welander et al., 2014b) using the GeneSpring GX v. 12.6 (Agilent, Santa Clara, CA) software and the Benjamini–Hochberg method (Benjamini and Hochberg, 1995) was used to control for multiple testing. When comparing the gene expression profiles between the 7 HRAS mutated cases and the 91 HRAS wild-type cases based on the entire probe sets on the array, a Benjamini–Hochberg corrected false discovery rate (FDR) of less than 0.1 was applied. Gene expression levels for HRAS, VEGFA, and PNMT were compared between sporadic HRAS-mutated and HRAS wild-type tumors using two-tailed Student's t-test. Two-tailed Mann–Whitney U or Fisher's exact tests were used to analyze potential significant correlations between the clinical parameters and HRAS mutational status. P-values of less than 0.05 were considered as statistically significant.

RESULTS

Detection of HRAS Mutations

A HRAS mutation was found in 11 out of 156 tumors screened (142 PCCs and 14 PGLs), equaling a total frequency of 7.1% (11/156) in our cohort (Table 1). One mutation was found in exon 2

TABLE 2. Summary of HRAS Mutation Studies in PPGL

	HRAS gene status						PPGL susceptibility gene	
	HRAS mutated	Codon 13 G13R	Codon 61 Q61R	Codon 61 Q61K	Codon 61 Q61L	Wild-type codon 13/61	Known mutation	Unknown mutation (sporadic)
This study[a]								
PCC (n = 141)	9	1	5	3	0	132	48	93
PGL (n = 14)	1	0	0	0	1	13	7	7
Total (n = 155)	10	1	5	3	1	145	55	100
Moley et al. 1991								
PCC (n = 10)	0	0	0	0	0	10	0	10
Total (n = 10)	0	0	0	0	0	10	0	10
Yoshimoto et al. 1992								
PCC (n = 19)	1	1	0	0	0	18	0	19
Total (n = 19)	1	1	0	0	0	18	0	19
Crona et al. 2013[b]								
PCC (n = 72)	3	1	1	1	0	69	22	50
PGL (n = 9)	1	0	1	0	0	8	3	6
Total (n = 81)	4	1	2	1	0	77	25	56
Oudijk et al. 2013								
PCC (n = 216)	14	1	12	1	0	202	76	140
PGL (n = 55)	0	0	0	0	0	55	31	24
Total (n = 271)	14	1	12	1	0	257	107	164
Luchetti et al. 2015[c]								
PCC (n = 60)	6	1	5	0	0	54	16	44
PGL (n = 5)	0	0	0	0	0	5	0	5
Total (n = 65)	6	1	5	0	0	59	16	49
Castro-Vega et al. 2015[d]								
PCC (n = 168)	10	1	4	2	0	158	100	68
PGL (n = 25)	0	0	0	0	0	25	16	9
Total (n = 193)	10	1	4	2	0	183	116	77
de Cubas et al. 2015								
PCC (n = 128)	3	0	3	0	0	125	68	60
PGL (n = 28)	1	0	0	1	0	27	15	13
Total (n = 156)	4	0	3	1	0	152	83	73
HRAS mutations in the eight studies								
PCC (n = 814)	**46 (5.7%)**	6 (0.7%)	30 (3.7%)	7 (0.9%)	0	768 (94.3%)	1/330 (0.3%)	45/484 (9.3%)
PGL (n = 136)	**3 (2.2%)**	0	1 (0.7%)	1 (0.7%)	1 (0.7%)	133 (97.8%)	0/72	3/64 (4.7%)
Total (n = 950)	**49 (5.2%)**	**6 (0.6%)**	**31 (3.3%)**	**8 (0.8%)**	**1 (0.1%)**	**901 (94.8%)**	**1/402 (0.2%)**	**48/548 (8.8%)**

[a]One PCC with a Q61R HRAS mutation has been previously published (Juhlin et al., 2015) and is excluded.
[b]One head and neck paraganglioma is excluded.
[c]Twenty head and neck paragangliomas are excluded.
[d]Six metastases and 3 thoracic paragangliomas are excluded. Three HRAS mutations from this study are not reported in the table: G12R (n = 1), S145L (n = 1), and A146T (n = 1).

(G13R) and ten mutations were found in exon 3 (six Q61R, three Q61K, and one Q61L) (Table 1, Fig. 1A).

The HRAS mutation frequency in apparently sporadic PPGL (non-familial and without known susceptibility gene mutation) was 10.9% (11/101; Table 1). The HRAS mutation status was compared with clinical and genetic characteristics of the present cohort and in combination with published studies (Table 1). No HRAS mutation was found in any PPGL endowed with a known PPGL susceptibility gene mutation (Table 1, Supporting Information Table 1). Hence, HRAS mutations were associated with the PPGL group without a known susceptibil-

ity gene mutation both in our study (Fisher's exact test, $P = 0.017$) (Table 1) and in all available studies combined (Fisher's exact test, $P < 0.0001$) (Table 2). Regarding clinical parameters, no mutations were found in PPGLs classified as malignant according to the current WHO criteria and the patients endowed with a HRAS mutation tended to have higher age at diagnosis (mean 63 ±10 years) compared with those without HRAS mutation (mean 54 ±16 years) however this association did not reach statistical significance (two-tailed Mann–Whitney U-test, $P = 0.08$). In our series of 11 mutated PPGLs there were four men and seven women, and no gender-related difference in HRAS

TABLE 3. Genes with Altered Expression in *HRAS* Mutated Tumors (*n* = 7) Compared with *HRAS* Wild-Type Cases (*n* = 91) using a Benjamini–Hochberg Corrected FDR of 10 %

Transcript cluster id	Corrected *P*-value	Fold change	Fold change log	Gene symbol
Up-regulated in *HRAS* mutated vs. wild-type				
8135774	0.0632	2.7526	1.4608	PTPRZ1
8138337	0.0000	2.3660	1.2424	TMEM195
7928907	0.0253	2.0682	1.0484	
8000963	0.0025	1.9834	0.9880	STX1B
7921852	0.0532	1.7622	0.8174	MPZ
8107518	0.0532	1.6164	0.6928	
8103374	0.0889	1.5410	0.6239	
8152863	0.0253	1.5150	0.5993	
8156110	0.0253	1.5148	0.5991	
8000757	0.0005	1.4531	0.5391	DOC2A
8157027	0.0253	1.4506	0.5367	NIPSNAP3B
7998053	0.0854	1.3622	0.4459	
7948037	0.0253	1.3206	0.4012	
7965838	0.0300	1.1981	0.2608	
8040672	0.0832	1.1767	0.2347	DRC1
Down-regulated in *HRAS* mutated vs. wild-type				
8036483	0.0909	−1.3839	−0.4687	YIF1B
8098705	0.0604	−1.3403	−0.4225	MTRF1L
8061542	0.0832	−1.3147	−0.3948	HM13
7989619	0.0419	−1.3038	−0.3827	PPIB
7983290	0.0253	−1.3018	−0.3805	SERF2
7924230	0.0832	−1.2333	−0.3025	ABHD17A

mutation frequency was observed (Fisher's exact test, $P = 0.76$). The mean tumor sizes of *HRAS*-mutated and wild-type cases were 58 ± 41 mm and 45 ± 22 mm, respectively. This difference was not statistically significant (Two-tailed Mann–Whitney *U*-test, $P = 0.37$).

mRNA Expression Profiles of *HRAS* Mutated PPGLs

Two approaches were taken to reveal gene expression profiles associated with the *HRAS* mutational status. First, hierarchical clustering was performed using the previously defined set of 454 probe sets (Burnichon et al., 2011). This showed that the seven *HRAS* mutated PPGL clustered together with the tumors endowed with mutations in the *NF1* and *RET* genes, associated with PIK3/AKT/mTOR and RAS/RAF activation in Cluster 2 (Fig. 1B). When *HRAS* mutated and *HRAS* wild-type cases were separately compared for the individual genes *HRAS*, *VEGFA*, and *PNMT*, the latter was found to have significantly higher expression in *HRAS*-mutated cases (Student's *t*-test, $P = 0.018$) (Fig. 1C) whereas *HRAS* and *VEGFA* did not show statistically significant differences between groups (Student's *t*-test, $P = 0.061$ and $P = 0.29$, respectively).

Subsequently, the 7 *HRAS* mutated tumors were compared with 91 *HRAS* wild-type tumors using the complete set of probe sets on the array. Based on this, 21 differentially expressed transcripts were identified as detailed in Table 3. Thirteen of the identified transcripts correspond to a known gene, including the *receptor-type tyrosine-protein phosphatase zeta (PTPRZ1)* and the *transmembrane protein 195 (TMEM195)* as the two most up-regulated genes.

DISCUSSION

In this study we aimed to further establish the *HRAS* mutation frequency in PPGL and examine the impact on global expressional profiles in *HRAS* mutated tumors. We consequently screened 156 PPGLs for mutations in the *HRAS* gene and compared the results with microarray-based gene expression profiles for 93 (60%) of the cases.

Eleven out of 156 cases were found endowed with *HRAS* mutations equaling a total frequency of 7.1%. This prevalence is in line with previously published results (Table 2) (Yoshimoto et al., 1992; Crona et al., 2013; Oudijk et al., 2014; Castro-Vega et al., 2015; Luchetti et al., 2015). One single mutation was found in exon 2 (G13R) and ten mutations were found in exon 3 (six Q61R, three Q61K and one Q61L). The Q61L mutation at c.182 A>T (COSM498), which has previously not been reported in PPGL, was the only mutation found in a PGL in our cohort. This alteration has previously been reported in cutaneous squamous cell carcinoma (Su et al., 2012) and in penile cancer (Andersson et al., 2008).

No *HRAS* mutations were found in PPGLs classified as malignant according to the current WHO criteria, which is in line with previous findings (Yoshimoto et al., 1992; Crona et al., 2013; Oudijk et al., 2014; Castro-Vega et al., 2015), however one single metastatic case with a *HRAS* mutation has been previously reported (de Cubas et al., 2015). The observed male:female proportion is in line with the results shown in two studies (Oudijk et al., 2014; Castro-Vega et al., 2015), but conflicting the results shown in an earlier study (Crona et al., 2013) where 4/4 patients with *HRAS* mutations were men. The mean tumor size of *HRAS*-mutated cases tended to be slightly increased as compared with *HRAS* wild-type cases (58 mm vs. 45 mm), however the difference was not statistically significant which is in agreement with the results of three preceding studies where the parameter was included (Crona et al., 2013; Oudijk et al., 2014).

None of the *HRAS* mutated tumors in our cohort were malignant according to the WHO criteria, suggesting a role of *HRAS* mutations as a somatic driver event in benign PPGL. As with the other genes associated with kinase signaling pathways in PPGL, *HRAS* mutations appear to be associated with a benign phenotype overall, although characterization and long term follow-up in additional cohorts will be required to determine if they may be used as predictive markers.

Activating mutations in the *HRAS* gene are known to affect MAPK signaling (Balmain and Pragnell, 1983), and as might be expected, all seven *HRAS* mutated cases included in the microarray-based profiling were grouped in Cluster 2 together with tumors harboring mutations in the *NF1, MAX, RET* and *TMEM127* genes associated with PIK3/AKT/mTOR and RAS/RAF activation. Taken together with preceding findings (Castro-Vega et al., 2015), these results support the notion that *HRAS*-mutated cases segregate separately from Cluster 1 tumors. Tumors with *HRAS* mutations exhibited higher expression of the *PNMT* gene encoding the PNMT enzyme that catalyzes the conversion (methylation) between norepinephrine and epinephrine. This finding is in line with a previous study showing that Cluster 2 tumors have increased *PNMT* expression and hence higher epinephrine levels in the patient (Eisenhofer et al., 2004). Interestingly, several tumors without mutations in any of the so far known susceptibility genes appear to form a group within Cluster 1 (Fig. 1B). An underlying somatic *VHL* mutation was excluded in these cases based on previous mutation screenings in all cases included in the microarray (Supporting Information Table S1). One may speculate that these tumors might share unknown underlying genetic mechanisms that potentially involve regulation of the hypoxia response, which may be an interesting subject for future studies.

Based on the analyses using the entire probe set on the array, *PTPRZ1* was found to be the most up-regulated gene in *HRAS* mutated PPGL compared with *HRAS* wild-type tumors (Table 3). This gene has been shown to regulate glioblastoma cell motility (Müller et al., 2003) and activation of PTPRZ1 via hypoxia inducible factor-2 alpha (HIF-2α) has also been suggested (Wang et al., 2010).

To summarize, we were able to establish a low *HRAS* mutation frequency (7.1%) in PPGL. Taken together with all other studies published up to date, the overall *HRAS* mutation prevalence in PPGL is 5.2% (49/950) and 8.8% (48/548) among apparently sporadic cases without a known PPGL susceptibility gene mutation. *HRAS* mutated cases were grouped into Cluster 2 and somatic *HRAS* mutations did not occur in patients with a known PPGL susceptibility gene mutation or in patients with malignant PPGL. Somatic *HRAS* mutations thus represent a possible driver event for a subset of benign PPGLs.

REFERENCES

Andersson P, Kolaric A, Windahl T, Kirrander P, Söderkvist P, Karlsson MG. 2008. PIK3CA, HRAS and KRAS gene mutations in human penile cancer. J Urol 179:2030–2034.

Andreasson A, Kiss NB, Caramuta S, Sulaiman L, Svahn F, Bäckdahl M, Höög A, Juhlin CC, Larsson C. 2013a. The VHL gene is epigenetically inactivated in pheochromocytomas and abdominal paragangliomas. Epigenetics 8:1347–1354.

Andreasson A, Kiss NB, Juhlin CC, Höög A. 2013b. Long-Term storage of endocrine tissues at −80°C does not adversely affect RNA quality or overall histomorphology. Biopreserv Biobank 11:366–370.

Balmain A, Pragnell IB. 1983. Mouse skin carcinomas induced in vivo by chemical carcinogens have a transforming Harvey-ras oncogene. Nature 303:72–74.

Benjamini Y, Hochberg Y. 1995. Controlling the false discovery rate: A practical and powerful approach to multiple testing. J R Stat Soc B Met 57:289–300.

Burnichon N, Vescovo L, Amar L, Libé R, de Reynies A, Venisse A, Jouanno E, Laurendeau I, Parfait B, Bertherat J, Plouin PF, Jeunemaitre X, Favier J, Gimenez-Roqueplo AP. 2011. Integrative genomic analysis reveals somatic mutations in pheochromocytoma and paraganglioma. Hum Mol Genet 20:3974–3985.

Cascón A, Comino-Méndez I, Currás-Freixes M, de Cubas AA, Contreras L, Richter S, Peitzsch M, Mancikova V, Inglada-Pérez L, Pérez-Barrios A, Calatayud M, Azriel S, Villar-Vicente R, Aller J, Setién F, Moran S, Garcia JF, Río-Machín A, Letón R, Gómez-Graña Á, Apellániz-Ruiz M, Roncador G, Esteller M, Rodríguez-Antona C, Satrústegui J, Eisenhofer G, Urioste M, Robledo M. 2015. Whole-exome sequencing identifies MDH2 as a new familial paraganglioma gene. J Natl Cancer Inst 11:107.

Castro-Vega LJ, Letouzé E, Burnichon N, Buffet A, Disderot PH, Khalifa E, Loriot C, Elarouci N, Morin A, Menara M, Lepoutre-Lussey C, Badoual C, Sibony M, Dousset B, Libé R, Zinzindohoue F, Plouin PF, Bertherat J, Amar L, de Reyniès A, Favier J, Gimenez-Roqueplo AP. 2015. Multi-omics analysis defines core genomic alterations in pheochromocytomas and paragangliomas. Nat Commun 6:6044.

Comino-Méndez I, Gracia-Aznárez FJ, Schiavi F, Landa I, Leandro-García LJ, Letón R, Honrado E, Ramos-Medina R, Caronia D, Pita G, Gómez-Graña A, de Cubas AA, Inglada-Pérez L, Maliszewska A, Taschin E, Bobisse S, Pica G, Loli P, Hernández-Lavado R, Díaz JA, Gómez-Morales M, González-Neira A, Roncador G, Rodríguez-Antona C, Benítez J, Mannelli

M, Opocher G, Robledo M, Cascón A. 2011. Exome sequencing identifies MAX mutations as a cause of hereditary pheochromo-cytoma. Nat Genet 43:663–667.

Crona J, Delgado Verdugo A, Maharjan R, Stålberg P, Granberg D, Hellman P, Björklund P. 2013. Somatic mutations in H-RAS in sporadic pheochromocytoma and paraganglioma identified by exome sequencing. J Clin Endocrinol Metab 98:E1266–E1271.

de Cubas AA, Korpershoek E, Inglada-Pérez L, Letouzé E, Currás-Freixes M, Fernández AF, Comino-Méndez I, Schiavi F, Mancikova V, Eisenhofer G, Mannelli M, Opocher G, Timmers H, Beuschlein F, de Krijger R, Cascon A, Rodríguez-Antona C, Fraga MF, Favier J, Gimenez-Roqueplo AP, Robledo M. 2015. DNA methylation profiling in pheochromocy-toma and paraganglioma reveals diagnostic and prognostic markers. Clin Cancer Res 21:3020–3030.

Dahia PLM. 2014. Pheochromocytoma and paraganglioma patho-genesis: Learning from genetic heterogeneity. Nat Rev Cancer 14:108–119.

Dahia PL, Ross KN, Wright ME, Hayashida CY, Santagata S, Barontini M, Kung AL, Sanso G, Powers JF, Tischler AS, Hodin R, Heitritter S, Moore F, Dluhy R, Sosa JA, Ocal IT, Benn DE, Marsh DJ, Robinson BG, Schneider K, Garber J, Arum SM, Korbonits M, Grossman A, Pigny P, Toledo SP, Nosé V, Li C, Stiles CD. 2005. A HIF1alpha regulatory loop links hypoxia and mitochondrial signals in pheochromocytomas. PLoS Genet 1:72–80.

DeLellis RA, Lloyd RV, Heitz PU, Eng C. 2004. World Health Organization Classification of Tumours. Pathology and Genetics of Tumours of Endocrine Organs. Lyon: IARC Press. pp. 147–166.

Eisenhofer G, Huynh T-T, Pacak K, Brouwers FM, Walther MM, Linehan WM, Munson PJ, Mannelli M, Goldstein DS, Elkahloun AG. 2004. Distinct gene expression profiles in nor-epinephrine- and epinephrine-producing hereditary and spo-radic pheochromocytomas: Activation of hypoxia-driven angiogenic pathways in von Hippel-Lindau syndrome. Endocr Relat Cancer 11:897–911.

Fishbein L, Khare S, Wubbenhorst B, DeSloover D, D'Andrea K, Merrill S, Cho NW, Greenberg RA, Else T, Montone K, LiVolsi V, Fraker D, Daber R, Cohen DL, Nathanson KL. 2015. Whole-exome sequencing identifies somatic ATRX muta-tions in pheochromocytomas and paragangliomas. Nat Commun 6:6140.

Juhlin CC, Stenman A, Haglund F, Clark VE, Brown TC, Baranoski J, Bilguvar K, Goh G, Welander J, Svahn F, Rubinstein JC, Caramuta S, Yasuno K, Günel M, Bäckdahl M, Gimm O, Söderkvist P, Prasad ML, Korah R, Lifton RP, Carling T. 2015. Whole-exome sequencing defines the muta-tional landscape of pheochromocytoma and identifies KMT2D as a recurrently mutated gene. Genes Chromosomes Cancer 54:542–554.

Letouzé E, Martinelli C, Loriot C, Burnichon N, Abermil N, Ottolenghi C, Janin M, Menara M, Nguyen AT, Benit P, Buffet A, Marcaillou C, Bertherat J, Amar L, Rustin P, De Reyniès A, Gimenez-Roqueplo AP, Favier J. 2013. SDH muta-tions establish a hypermethylator phenotype in paraganglioma. Cancer Cell 23:739–752.

Liu T, Brown TC, Juhlin CC, Andreasson A, Wang N, Bäckdahl M, Healy JM, Prasad ML, Korah R, Carling T, Xu D, Larsson C. 2014. The activating TERT promoter mutation C228T is recurrent in subsets of adrenal tumors. Endocr Relat Cancer 21:427–434.

Luchetti A, Walsh D, Rodger F, Clark G, Martin T, Irving R, Sanna M, Yao M, Robledo M, Neumann HP, Woodward ER, Latif F, Abbs S, Martin H, Maher ER. 2015. Profiling of somatic mutations in phaeochromocytoma and paraganglioma by targeted next generation sequencing analysis. Int J Endocri-nol 2015:138573.

Moley JF, Brother MB, Wells SA, Spengler BA, Biedler JL, Brodeur GM. 1991. Low frequency of ras gene mutations in neuroblastomas, pheochromocytomas, and medullary thyroid cancers. Cancer Res 51:1596–1599.

Müller S, Kunkel P, Lamszus K, Ulbricht U, Lorente GA, Nelson AM, von Schack D, Chin DJ, Lohr SC, Westphal M, Melcher T. 2003. A role for receptor tyrosine phosphatase zeta in glioma cell migration. Oncogene 22:6661–6668.

Oudijk L, de Krijger RR, Rapa I, Beuschlein F, de Cubas AA, Dei Tos AP, Dinjens WN, Korpershoek E, Mancikova V, Mannelli M, Papotti M, Vatrano S, Robledo M, Volante M. 2014. H-RAS mutations are restricted to sporadic pheochromo-cytomas lacking specific clinical or pathological features: Data from a multi-institutional series. J Clin Endocrinol Metab 99: E1376–E1380.

Schlisio S, Kenchappa RS, Vredeveld LC, George RE, Stewart R, Greulich H, Shahriari K, Nguyen NV, Pigny P, Dahia PL, Pomeroy SL, Maris JM, Look AT, Meyerson M, Peeper DS, Carter BD, Kaelin WG. Jr. 2008. The kinesin KIF1Bbeta acts downstream from EglN3 to induce apoptosis and is a potential 1p36 tumor suppressor. Genes Dev 22:884–893.

Su F, Viros A, Milagre C, Trunzer K, Bollag G, Spleiss O, Reis-Filho JS, Kong X, Koya RC, Flaherty KT, Chapman PB, Kim MJ, Hayward R, Martin M, Yang H, Wang Q, Hilton H, Hang JS, Noe J, Lambros M, Geyer F, Dhomen N, Niculescu-Duvaz I, Zambon A, Niculescu-Duvaz D, Preece N, Robert L, Otte NJ, Mok S, Kee D, Ma Y, Zhang C, Habets G, Burton EA, Wong B, Nguyen H, Kockx M, Andries L, Lestini B, Nolop KB, Lee RJ, Joe AK, Troy JL, Gonzalez R, Hutson TE, Puzanov I, Chmielowski B, Springer CJ, McArthur GA, Sosman JA, Lo RS, Ribas A, Marais R. 2012. RAS mutations in cutane-ous squamous-cell carcinomas in patients treated with BRAF inhibitors. N Engl J Med 366:207–215.

Wadt K, Choi J, Chung JY, Kiilgaard J, Heegaard S, Drzewiecki KT, Trent JM, Hewitt SM, Hayward NK, Gerdes AM, Brown KM. 2012. A cryptic BAP1 splice mutation in a family with uveal and cutaneous melanoma, and paraganglioma. Pigment Cell Melanoma Res 25:815–818.

Wang V, Davis DA, Veeranna RP, Haque M, Yarchoan R. 2010. Characterization of the activation of protein tyrosine phospha-tase, receptor-type, Z polypeptide 1 (PTPRZ1) by hypoxia inducible factor-2 alpha. PLoS One 5:9641.

Welander J, Andreasson A, Juhlin CC, Wiseman RW, Bäckdahl M, Höög A, Larsson C, Gimm O, Söderkvist P. 2014a. Rare germline mutations identified by targeted next-generation sequencing of susceptibility genes in pheochromocytoma and paraganglioma. J Clin Endocrinol Metab 99:1352–1360.

Welander J, Andreasson A, Brauckhoff M, Bäckdahl M, Larsson C, Gimm O, Söderkvist P. 2014b. Frequent EPAS1/HIF2α exons 9 and 12 mutations in non-familial pheochromocytoma. Endocr Relat Cancer 21:495–504.

Yoshimoto K, Iwahana H, Fukuda A, Sano T, Katsuragi K, Kinoshita M, Saito S, Itakura M. 1992. ras mutations in endo-crine tumors: Mutation detection by polymerase chain reaction-single strand conformation polymorphism. Jpn J Cancer Res Gann 83:1057–1062.